Journal of the European Ceramic Society 15 (1995) 983–988

0955-2219(95)00070-4
0955-2219/95/$9.50

Microstructure and Creep Properties of Alumina/Zirconia Ceramics

José María Calderón-Moreno,[a] Antonio R. de Arellano-López,[a] Arturo Domínguez-Rodríguez[a] & Jules L. Routbort[b]

[a]Departamento de Física de la Materia Condensada & Instituto de Ciencias de Materiales de Sevilla, Universidad de Sevilla-CSIC, Sevilla, Spain
[b]Materials Science Division, Argonne National Laboratory, Argonne, Illinois 60439, USA

(Received 18 May 1994; revised version received 20 March 1995; accepted 31 March 1995)

Abstract

High temperature creep of two zirconia toughened alumina ceramics, fabricated by powder processing and sol–gel precursors processing, has been studied in order to determine plastic deformation mechanisms. Compressive creep tests were carried out between 1300 and 1450°C, under stresses from 10 to 150 MPa. For the sample fabricated from powders, a stress exponent of 1·4 and an activation energy of 580 kJ/mol were found below a critical stress of 40 MPa. For larger stresses, accelerated creep rates developed. In the specimens processed from precursors, values of 1·8 for the stress exponent and 540 kJ/mol for the activation energy, over the entire range of stresses have been determined. Creep parameters and microstructural evolution of the samples during the experiments have been correlated with models to establish the dominant creep mechanism.

Introduction

ZrO_2 has a very high fracture toughness and its addition to other ceramics, zirconia toughened ceramics (ZTC), has many advantages.[1] In the last eighteen years, a number of investigations of the mechanical and microstructural features of ZTCs, in particular in the system Al_2O_3–ZrO_2, also called zirconia toughened alumina, ZTA, have been performed.[2,3] The major application of ZTAs has been metal cutting tools.[4]

Available results on mechanical properties of ZTA are mainly on fracture, strength, and elasticity. All properties show a strong dependence on the volume fraction of each component, on the ratio of tetragonal and monoclinic zirconia, as well as on zirconia grain size (GS). The review by Green *et al.*,[5] summarizes most of these results.

Fracture studies[3] on ZTA, have shown an increase in K_{Ic} (up to 10 MPa.m$^{1/2}$) with increasing zirconia volume fraction, in particular for small grain sizes (< 1 μm). These authors have claimed that the total increment in fracture toughness is a combination of transformation and microcrack mechanisms of toughening. The first is only possible if t-ZrO_2 particles are present, and the second actuates if zirconia particles at the grain boundaries are transformed to monoclinic by cooling down from the sintering temperature.

In some cases, microcracking resulted in a reduction of strength which is particularly deleterious for large zirconia GS, and volume percentages.[6] To avoid flaws, some researchers have HIP-ed sintered samples,[6] and obtained improved strength, in particular for t-ZrO_2. Some improvement in flexural strength has been also reported for volume percentages of mainly t-ZrO_2 up to 10%.[3] Other authors have studied the retained strength after thermal shock.[7] A sharp decrease in this parameter occurs if samples are heated over the phase transformation temperature and then cooled down. Both room-temperature Vickers hardness, and Young's modulus decrease with increasing zirconia content, in particular, in specimens with high microcracking activity.[8]

In this study our objective is to obtain knowledge on plastic deformation mechanisms in composite systems, as well as on the microstructural effects of creep. Only a few high-temperature mechanical properties data are available. Due to such lack of data, we will compare our results with related materials, like monolithic Al_2O_3 or ZrO_2.

Experimental Techniques

(a) Material

Creep of two polycrystalline ZTA ceramics with 94·5 vol% of Al_2O_3 and 5·5 vol% of ZrO_2 has been

studied. In one case, processing was conducted by wet mixing of powder raw materials and dispersants. The alumina was in the form of α-Al_2O_3 and the zirconia powder was of high purity (99·995%), in the form of monoclinic m-ZrO_2, with a typical particle size of 0·5 μm. Densification took place after drying by uniaxial hot-pressing, at 1600°C, achieving full density. This type of material will be called pd-ZTA.

In the other materials, the processing was carried out by a sol–gel technique using an Al_2O_3 solution and a ZrO_2 precursor, which should result in a better mixing of components. After calcination, screening and drying, uniaxial hot-pressing was performed at 1600°C, obtaining fully dense samples. Throughout this paper, this material will be called pc-ZTA.

(b) Mechanical testing

Mechanical tests have been carried out under compression on 3 × 3 × 5 mm^3 samples, both at constant strain rate (CSR) of 1·7 × 10^{-5} s^{-1}, and or constant load (CL) between 10 and 150 MPa (engineering stress). Temperatures ranged from 1300 to 1450°C. All tests were performed in air.

(c) Microstructural observations

Polished surfaces of as-received and deformed samples were observed by SEM. Some were thermally etched in air at 1450°C to reveal grain morphology. Several microstructural parameters (zirconia distribution, GS, and shape) were studied by means of an image analyzer.

Other microstructural features (dislocations, cracks,...), have been studied by TEM in as-received and deformed specimens. TEM samples were prepared using standard techniques and were carbon coated before observation.

Microstructure of As-Received Samples

(a) ZTA prepared from powders

ZrO_2 grains are homogeneously distributed throughout the Al_2O_3 matrix, with a typical log–normal distribution of GS. 20% of the total volume fraction of zirconia are small particles (<0·5 μm) and are normally embedded in large alumina grains having an average GS of 4·7 ± 0·7 μm, as seen by TEM (Fig. 1). Another 60% of ZrO_2 are grains between 0·5 and 7 μm diameter, located at grain boundaries (GB) and triple point junctions. Finally, the remaining 20% of ZrO_2 are large conglomerates (>7 μm, with a maximum size of 38 μm) located between Al_2O_3 grains. These conglomerates have a lenticular shape oriented perpendicularly to the hot-pressing axis (HPA) (Fig. 2).

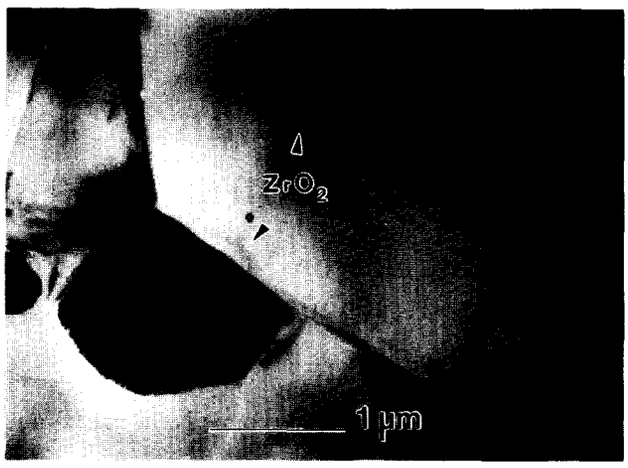

Fig. 1. TEM micrograph of pd-ZTA showing small zirconia particles.

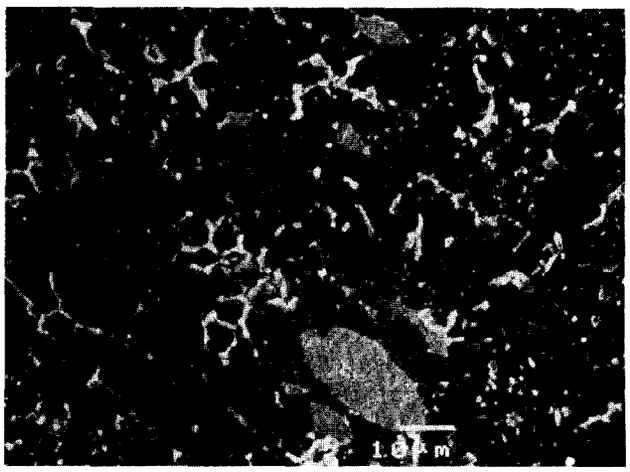

Fig. 2. SEM micrograph of polished pd-ZTA showing alumina GS and one of the lenticular agglomerates of zirconia oriented perpendicularly to the HPA axis.

Several studies have reported similar microstructures. Kibbel and Heuer,[9,10] for instance, indicated that the presence of zirconia, enhances in some cases the growth of alumina usually resulting in small-trapped ZrO_2 particles. Heuer *et al.*[11] showed that trapped grains, with GS smaller than 0·5 μm, are mostly tetragonal, and are very unlikely to transform to monoclinic in a rigid matrix like Al_2O_3,[12] while larger particles, normally placed at grain boundaries, are mainly monoclinic. When the dispersion of zirconia in matrix is not good enough, the monoclinic particles can agglomerate, and form the larger particles reported in this and other studies.[13]

The effect of the m-ZrO_2 along grain boundaries promotes poor thermal shock resistance. When heated up for sintering, etching or creep-testing, m-particles transform to tetragonal (over 1100°C for undoped zirconia). When cooled-down, they become monoclinic again, creating cracks, in particular around the large ZrO_2 particles previously mentioned.[7,8]

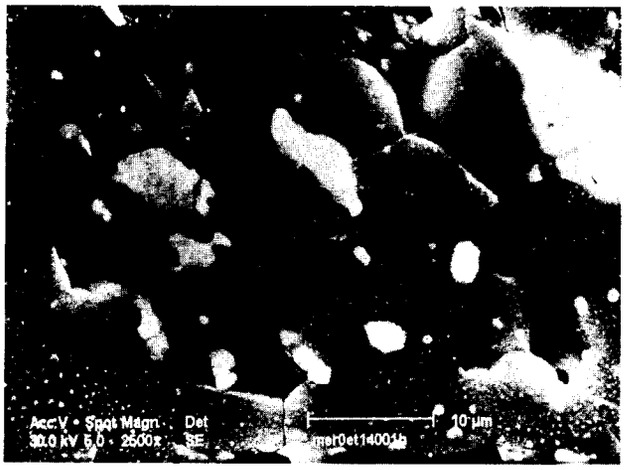

Fig. 3. SEM micrograph of polished and etched pd-ZTA showing a crack inbetween zirconia grains, and significant pull-out, due to microcracking.

In Fig. 3, a SEM micrograph taken on a polished and thermally etched surface, it is easy to observe the formation of extensive cracks between the large ZrO_2 particles. All observations confirm the activity of the martensitic transformation during etching, and, in general, during any thermal cycling over the transformation temperature.

The microstructure of the ZTA prepared by powder techniques is, therefore, 'intragranular–tetragonal/intergranular–monoclinic' as expected from all the above mentioned investigations.[1]

(b) ZTA prepared from precursors

In these samples, ZrO_2 particles are also homogeneously distributed through the matrix (Fig. 4). Nevertheless, an observed major difference compared with pd-ZTA is a much narrower log–normal distribution of zirconia grains, with 95% of the total number of particles smaller than 1 μm, mostly embedded into the Al_2O_3 grains which average a GS of $2{\cdot}6 \pm 0{\cdot}3$ μm.

When the samples were polished and etched for microstructural analysis, the features of grain pull-out, and microcracking due to thermal cycling, were not observed as in pd-samples. The absence of large monoclinic zirconia grains is responsible for this better microstructure. The ZrO_2 grains are small enough, even if they are located at grain boundaries, to keep their tetragonal structure. Therefore, we can characterize this pc-ZTA as 'intra-granular tetragonal'.[1]

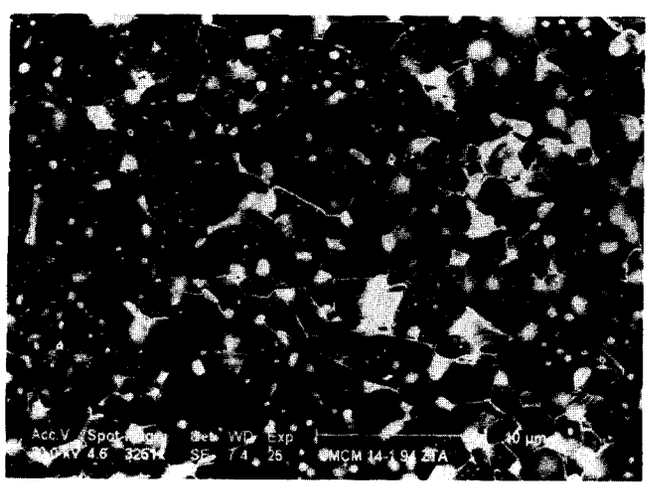

Fig. 4. SEM micrograph of pc-ZTA, showing the homogeneous GS and distribution of zirconia particles, and alumina GS.

Results

Figures 5 and 6 show results of CSR tests on pd-ZTA and pc-ZTA. At 1300 and 1350°C the samples fractured after 6–7% deformation. At the lower temperature strain/stress plots showed brittle fracture for σ = 385 MPa for pd-ZTA, and 434 MPa for pc-ZTA, while at 1350°C the samples fracture for σ = 231 MPa and 296 MPa, respectively, but exhibited plastic behavior. At 1400°C, 95 MPa was reached without fracture after 8% strain for the powder-processed samples. Some softening is detected in the final part of the plot, but without failure. Such behavior was also

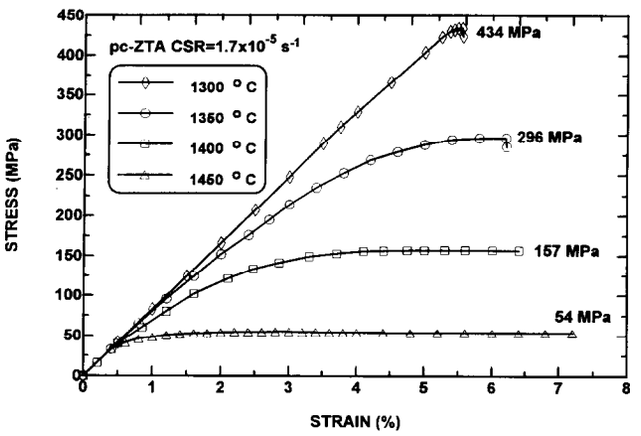

Fig. 5. Results of constant strain rate tests on pc-ZTA at different temperatures as shown.

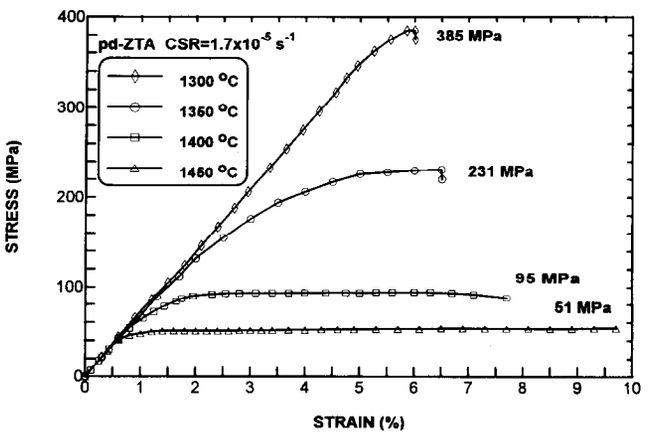

Fig. 6. Results of constant strain rate tests on pd-ZTA at different temperatures as shown.

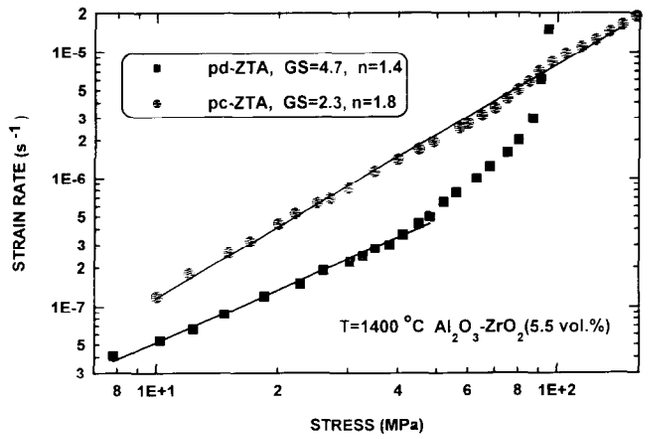

Fig. 7. Steady state strain rates reached on constant load tests versus true stresses.

observed in the tests performed on the precursor-processed samples, with a zero-work hardening stress of 157 MPa, in this case. At this last temperature, several CL tests were performed on different samples. For increasing stresses from 10 to 150 MPa, strain rates ranged between 4×10^{-8} and 2×10^{-5} s^{-1}. Steady-state strain rates are plotted in Fig. 7 versus the applied stress. The effect of temperature on creep rate, at constant load was studied between 1300 and 1450°C. An Arrhenius plot of (ln $\dot{\epsilon}$) versus (1/T) is shown in Fig. 8.

All of these results are analyzed using the phenomenological equation:

$$\dot{\epsilon} = A\sigma^n d^{-p}{}_{\exp}(-Q/RT) \qquad (1)$$

where $\dot{\epsilon}$ is the strain rate, σ is the stress, d is the grain size, A is a constant, and R and T have their usual meaning. The parameters n (stress exponent) and Q (activation energy) and p (grain size exponent) can be determined and correlated with plastic deformation mechanisms.

For the pd-ZTA material, two regimes of deformation were detected, with a change in the stress exponent from 1·4 ± 0·2 at low stresses, to variable values larger than two for higher stresses.

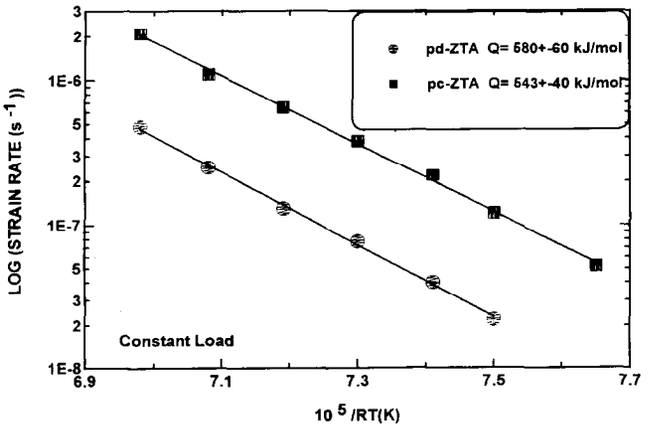

Fig. 8. Steady state strain rates reached on constant load tests versus (1/RT) in an Arrhenius plot.

The critical σ_c is above 40 MPa. On the other hand, in the range of stresses studied, a constant n = 1·8 ± 0·2 is measured for the pc-ZTA material.

We have determined the activation energy, Q, for both materials. 580 ± 60 kJ/mol is obtained for pd-ZTA, under 23 MPa ($< \sigma_c$), and 540 ± 40 kJ/mol for pc-ZTA, under 25 MPa.

However, in a complex material, like the one in this study, the meaning of these parameters in terms of creep mechanisms, is not clear without analyzing the microstructural evolution of the samples during plastic deformation. A complete discussion will follow.

Microstructural analysis was performed on samples deformed at 1400°C, from both CSR and CL tests. After the test, CSR deformed specimens showed extensive intergranular cracking. We can also see large cracks formed by coalescence of pre-existing cavities near ZrO_2 particles at grain boundaries (Fig. 9). After the CL experiments, we only observed samples deformed in the n = 1·4–1·8 regime. Some cavities were observed. However they should not control plastic deformation because it was possible to measure quasi-steady states of creep. A more detailed analysis of the role of cavitation in the creep of composite ceramics is out of the scope of this paper.

Grain size and morphology of deformed samples was studied. Neither alumina, nor zirconia grains appear to suffer major geometric changes. GS remains constant. The grains form factors, defined as

$$FF = 4\pi.(\text{area})/(\text{perimeter})^2,$$

remains around 0·8 up to 20% strain.

Discussion

For the compression rate used, with $T < 1400$°C,

Fig. 9. Cracks formed by coalescence of cavities developed at the surroundings of zirconia particles at grain boundaries during plastic deformation.

the pc-ZTA samples suffer brittle fracture at stresses typically higher than the ones measured for pd-ZTA samples. For temperatures over 1400°C both kinds of samples are plastic.

We have specifically studied plasticity at 1400°C, using a wide range of stresses. pc-ZTA specimens show a single deformation regime characterized by n = 1·8 and Q = 540 kJ/mol, while for pd-ZTA samples two regimes have been detected. In these samples, below $\sigma_c \approx 40$ MPa, approximately, the plastic deformation mechanisms is characterized by a sequence of steady states with calculated n = 1·4 and Q = 560 kJ/mol. For $\sigma > \sigma_c$ values for n and Q have little meaning. This non-steady state regime is a consequence of coalescence of cavities whose origin we have not investigated and will not be considered in the following analysis.

Absolute values of the strain-rate are between 2 and 5 times faster in pc-materials than in pd-samples, but this can be explained, in the light of eqn (1), by the difference in GS (d). If the $\dot{\epsilon}$ values are normalized for grain size differences using p = 2 or 3, the strain rates become, within the experimental scatter, equal. Figure 10 shows such a comparison for p = 2, for illustrational purposes. Also included in Fig. 10 is a comparison with results of a monolithic alumina of 3·3 μm GS, reported in a previous work.[14] Good concordance is found in the stress exponent (1·3 ± 0·1) and in the activation energy (510 ± 20 kJ/mol), and in the normalized strain rates (also included in Fig. 10). The accord might suggest that diffusion in both ZTA and Al_2O_3 is extrinsically controlled. The most important conclusion though is that no significant improvement in creep resistance in the steady-state region for either material is found.

The unchanged form factors indicate that grain boundary sliding (GBS)[15] is the dominant mechanisms of deformation since a pure diffusion mechanism requires a change of grains' shape. Additionally, large cracks can nucleate from

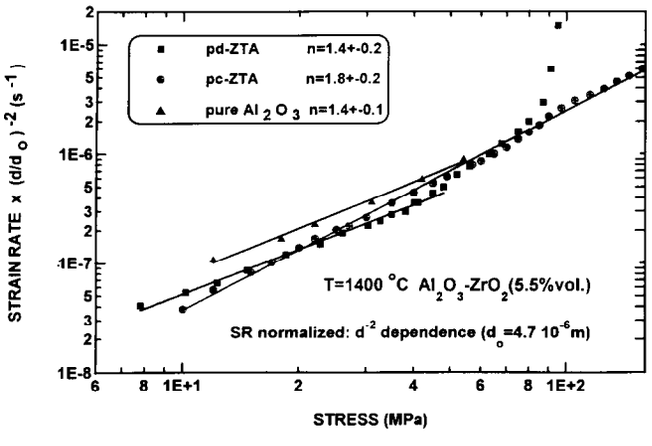

Fig. 10. Steady state strain rates normalized using p = 2, for a common grain size of 4·7 μm, for pd-ZTA, pc-ZTA and monoclinic alumina.[15]

ZrO_2-related microcracks, and will limit the utility of these materials over a certain critical strain (ϵ_c).

There are two mechanisms of diffusion accommodated GBS creep.[16] One is the mechanisms known as interface-reaction controlled (IRC) grain boundary sliding (with n = 2) and the other is transport of matter controlled (TMC) grain boundary sliding (n = 1), the first is more active in polycrystals with small grains. The creep parameter p can be either 2 or 3 in TMC creep, depending on the path of the creep controlling diffusion (p = 2 for lattice diffusion and p = 3 for grain boundary diffusion). In IRC creep the grain size exponent aries from 1 to 3. Both IRC and TMC, have been used to describe GBS in pure alumina[16,17] The parameter p in Al_2O_3 was found to be between both theoretical extremes, 2 and 3.

A range of n's from 1·1 to 2, and Q values from 410 to 568 kJ/mol has been reported in polycrystalline alumina specimens.[18] Although there is a general agreement that GBS is the dominant mechanism in Al_2O_3, there is much controversy on the meaning of the measured activation energies in terms of controlling diffusion species. Most authors claim that the higher values of Q are related to the diffusion of O^{2-} through the lattice, which is in agreement with p = 2, and has been detected in samples with large grain sizes (> 5 μm). On the other hand, the lower values of Q are claimed to result from grain boundary diffusion of Al^{3+}. A value of p = 3 is reported in these cases, usually found in samples with small grain sizes. However, comparisons are difficult because diffusion dynamics can be seriously altered by the presence of impurities,[19] and these are unknown in our samples. Our calculated creep parameters for ZTA, are consistent with the values reported for monolithic alumina. The values of n, and the microstructural observations, agree with the mechanism of unaccommodated GBS, with a mix of IRC and TMC. The largest values of n = 1·8, is found for the samples with the smallest grain size, and the lower n = 1·4 is found for samples with the largest grain size, in good agreement with predictions. The high values of Q found in this study support the control of the creep by O^{2-}, and the lattice is very likely to be the path of this transport of matter.

ZrO_2 agglomerates at grain boundaries are probably the origin of damage, and limit the strain to failure. The samples processed using the precursors technique contain less of these particles, and even though the unaccommodated GBS causes the formation of cavities, the samples remain intact with up to 40% strain. On the other hand, powder processed samples, which contains large zirconia particles, exhibit a critical stress over which the samples fail.

Baddi *et al.*[20] have studied the diffusional creep regime in a material of symmetric composition to the one in our work (zirconia matrix with alumina inclusions) and found that at low stresses IRC–GBS was dominating, while a TMC–GBS was active for the high stress range. Their microstructural analysis showed significant changes in the shape of the grains, without any cavitation. Other authors have proposed the same mechanisms (superplastic) acting in monolithic zirconia. The activation energy determined by Baddi and co-authors, also agreed with the one reported for monolithic zirconia In the material studied by Baddi *et al.*, the dominant component is then ZrO_2.

In our materials, it appears then, that the controlling component which determines the creep response is the harder phase: alumina. The role of the ZrO_2 phase is important in the brittle behavior and probably plays a role in the damage which accumulates in the plastic regime.

The better dispersion of the zirconia into the matrix in pc-TA, avoiding the formation of large intergranular monoclinic particles, results in better high-temperature mechanical response

Conclusions

It has been shown that the addition of 5·5 vol% of zirconia particles to an alumina matrix does not improve its resistance to creep. Creep takes place by grain boundary sliding and is accompanied by the formation of cavities. In the pd-samples, where large m-zirconia grains are present at grain boundaries, the linkage of the cavitation is easier because the inherent microcracking present in the samples, and results in a limited strain to failure and in a critical stress over which the formation of damage is too severe to allow measuring steady states of creep. On the other hand, for pc-samples, where a narrower GS distribution of smaller t-ZrO_2 particles has been measured, a single plastic regime of steady-states was detected. Cavities are also present in these crept samples, but the less microcracking activity promotes a better mechanical response.

We may conclude that the precursors-processed ZTA, with less microcracking, is a better candidate for high temperature applications than powder-processed ZTA, where microcracking is introduced by the presence of monoclinic zirconia grains.

Acknowledgements

The authors thank Lori Leaskey, from MER Corporation, Phoenix, Arizona, for supplying the samples. The work in Spain was supported by CICYT Project MAT91-0978 of the Spanish Ministerio de Educación y Ciencia. JLR was supported by the US Department of Energy, BES, Division of Materials Science under contract W-31-109-ENG.

References

1. Claussen, N., Microstructural design of zirconia-toughened ceramics. In *Science and Technology of Zirconia II, Advances in Ceramics*, vol. 12, eds N. Claussen, M. Rühle & A. H. Heuer. American Ceramic Society, Columbus, Ohio, 1984, pp. 325.
2. Claussen, N., Fracture toughness of Al_2O_3 with an unstabilized ZrO_2 dispersed phase, *J. Am. Ceram. Soc.*, **59** (1976) 49.
3. Claussen, N., Steeb, J. & Pabst, R. F. Effects of induced microcracking on fracture toughness of ceramics. *Am. Ceram. Soc. Bull.*, **56** (1977) 559.
4. Garvie, R. C., Microstructure and performance of an alumina–zirconia tool-kit, *J. Mat. Sci. Lett.*, **3** (1984) 315.
5. Green, D. J., Hannick, R. H. J. & Swain, M. V. In *Transformation toughening of ceramics*, CRC Press, Boca Raton, (1989), pp. 157–92.
6. Hori, S., Yoshimura, M. & Somiya S., Strength-toughness relations in sintered and isostatically hot-pressed ZrO_2 toughened Al_2O_3, *J. Am. Ceram. Soc.*, **69**(3) (1986) 169.
7. Becher, P. F., Transient thermal stress behaviour in ZrO_2–toughened Al_2O_3, *J. Am. Ceram. Soc.*, **64** (1981) 37.
8. Green, D. J., Critical microstructure for microcracking in Al_2O_3–ZrO_2 composites, *J. Am. Ceram. Soc.*, **65** (1982) 610.
9. Kibbel, B., Heuer, A. H., Ripening of inter- and intragranular ZrO_2–Toughened Al_2O_3. In *Science and Technology of Zirconia II, Advances in Ceramics*, vol. 12, eds N. Claussen, M. Rühle & A. H. Heuer, American Ceramic Society, Columbus, Ohio, (1984), pp. 415.
10. Kibbel, B. & Heuer, A. H., Exaggerated grain growth in ZrO_2–Toughened Al_2O_3, *J. Am. Ceram. Soc.*, **69** (1986) 231.
11. Heuer, A. H., Claussen, N., Kriven, W. M. & Rühle, M., Stability of tetragonal ZrO_2 particles in ceramic matrices, *J. Am. Ceram. Soc.*, **65**(12) (1982) 642.
12. Yuan, L. J. & Yen, T. S., Major influences on the particle size–transformation temperature relation in Al_2O_3–ZrO_2 composites, *J. Am. Ceram. Soc.*, **75**(9) (1992) 2576–80.
13. Witek, S. R. & Butler, E. P., Zirconia particle coarsening and the effects of zirconia additions on the mechanical properties of certain commercial aluminas, *J. Am. Ceram. Soc.*, **69**(7) (1986) 523.
14. DeArellano-López, A. R., Cumbrera, F. L., Domínguez-Rodriguez, A., Goretta, K. & Routbort J., Compressive creep of SiC-whisker-reinforced Al_2O_3, *J. Am. Ceram. Soc.*, **73**(5) (1990) 1297.
15. DeArellano-López, A. R., Domínguez-Rodriguez, A., Goretta, K. & Routbort, J., Plastic deformation mechanisms in SiC-whiskers-reinforced alumina, *J. Am. Ceram. Soc.*, **76**(6) (1993) 1425.
16. Ashby, M. F. & Verrall, R. A., Diffusional flow and superplasticity, *Acta Metall.*, **21** (1973) 149.
17. Cannon, R. M., Rhodes, W. H. & Heuer, A. H., Plastic deformation of fine grained Al_2O_3. I: Interface-controlled diffusional creep, *J. Am. Ceram. Soc.*, **63**(1–2) (1980) 46.
18. Heuer, A. H., Tighe, N. J. & Cannon, R. M., Plastic deformation of fine grained Al_2O_3. II: Basal slip and unaccommodated grain boundary sliding, *J. Am. Ceram. Soc.*, **63**(1–2) (1980) 53.
19. Castaing J., Domínguez-Rodríguez, A. & Monty, C., Oxygen diffusion and its relationship to high-temperature deformation of ceramic oxides, *Jpn. J. Appl. Phys., Ser. 2*, **28** (1989) 97–103.
20. Baddi, R., Clarisse, L., Duclos, R. & Crampon, J., Diffusional creep of alumina–zirconia composites: mechanical behavior and microstructure. In *Third Euroceramics*, vol. 3, eds P. Durán & J. F. Fernández, Faenza Editorial, Spain, (1993), pp. 641–6.